

Video Article

Lensfree On-chip Tomographic Microscopy Employing Multi-angle Illumination and Pixel Super-resolution

Serhan O. Isikman¹, Waheb Bishara¹, Aydogan Ozcan^{1,2,3}¹Electrical Engineering Department, University of California, Los Angeles²Bioengineering Department, University of California, Los Angeles³California NanoSystems Institute, University of California, Los AngelesCorrespondence to: Aydogan Ozcan at ozcan@ucla.eduURL: <http://www.jove.com/video/4161/>

DOI: 10.3791/4161

Keywords: Bioengineering, Issue 66, Electrical Engineering, Mechanical Engineering, lensfree imaging, lensless imaging, on-chip microscopy, lensfree tomography, 3D microscopy, pixel super-resolution, *C. elegans*, optical sectioning, lab-on-a-chip

Date Published: 8/16/2012

Citation: Isikman, S.O., Bishara, W., Ozcan, A. Lensfree On-chip Tomographic Microscopy Employing Multi-angle Illumination and Pixel Super-resolution. *J. Vis. Exp.* (66), e4161 10.3791/4161, DOI : 10.3791/4161 (2012).

Abstract

Tomographic imaging has been a widely used tool in medicine as it can provide three-dimensional (3D) structural information regarding objects of different size scales. In micrometer and millimeter scales, optical microscopy modalities find increasing use owing to the non-ionizing nature of visible light, and the availability of a rich set of illumination sources (such as lasers and light-emitting-diodes) and detection elements (such as large format CCD and CMOS detector-arrays). Among the recently developed optical tomographic microscopy modalities, one can include optical coherence tomography, optical diffraction tomography, optical projection tomography and light-sheet microscopy.¹⁻⁶ These platforms provide sectional imaging of cells, microorganisms and model animals such as *C. elegans*, zebrafish and mouse embryos.

Existing 3D optical imagers generally have relatively bulky and complex architectures, limiting the availability of these equipments to advanced laboratories, and impeding their integration with lab-on-a-chip platforms and microfluidic chips. To provide an alternative tomographic microscope, we recently developed lensfree optical tomography (LOT) as a high-throughput, compact and cost-effective optical tomography modality.⁷ LOT discards the use of lenses and bulky optical components, and instead relies on multi-angle illumination and digital computation to achieve depth-resolved imaging of micro-objects over a large imaging volume. LOT can image biological specimen at a spatial resolution of $<1 \mu\text{m} \times <1 \mu\text{m} \times <3 \mu\text{m}$ in the x, y and z dimensions, respectively, over a large imaging volume of 15-100 mm³, and can be particularly useful for lab-on-a-chip platforms.

Video Link

The video component of this article can be found at <http://www.jove.com/video/4161/>

Protocol

1. Imaging Setup

LOT can be assembled in a compact and lightweight field-portable architecture⁸, and alternatively as an optofluidic microscope with sectional imaging ability.⁹ In this report, however, we will describe the basic imaging setup for a bench-top implementation toward tomography of static samples.

1. **Illumination Module:** In LOT, partially coherent light sources such as light-emitting-diodes (LEDs) can be utilized. For experimental flexibility, we used a monochromator with a Xenon lamp (Cornerstone T260, Newport Corp.). The monochromator was adjusted to provide an output with ~1-10 nm spectral width around a center wavelength of e.g. 450-650 nm. This partially coherent output is then coupled to a multimode optical fiber (Thorlabs AFS105/125Y) to deliver partially coherent light to the system.

The optical fiber is mounted on a motorized rotation stage (Thorlabs PRM-1Z8 driven by Thorlabs TDC001 controller) to change the angle of illumination. The motorized stage, with the light source attached, is mounted on a two-dimensional linear X-Y stage (Newport ILS50CC driven by Newport MFA-PPD controllers), which was used to achieve in-plane shifts of the light source at a given angle.

2. **Detection:** Lensfree optical tomography is a scalable technology such that the detector array can be chosen according to the requirements of the applications without significantly changing the image acquisition steps or the data processing. In this report, we employed a CMOS sensor array having 5 Mega Pixels, with a pixel size of 2.2 μm (IDS Imaging, UI-1485LE-M). The detector is used to record the wide field-of-view (e.g. 24 mm²) holographic images of samples, which were placed directly on the top of the active area of the detector. If a dual-axis

tomography setup is to be implemented⁷, the detector should also be mounted on a horizontal (with respect to the optical table) rotation stage (e.g. Thorlabs RP-01) to rotate the sample (together with the detector) in the plane normal to the optic axis.⁷

2. Sample Preparation

While lensfree optical tomography can image a variety of objects such as cells and microorganisms, we will illustrate the basic principles by performing three-dimensional microscopy of a *C. elegans* sample.

1. Using a scalpel or a spatula, take a small piece of agar from the Petri dish containing the *C. elegans* culture. A cubic piece of several millimeters along each dimension will contain hundreds of nematodes.
2. Place the small chunk of agar in a polypropylene vial containing 1 ml de-ionized (DI) water.
3. Gently vortex for 0.5-1 min, and wait for 10-15 min until the worms crawl out of the agar piece into the DI water.
4. In order to temporarily immobilize the worms, add 1 ml of 5-10 mM levamisole solution (Sigma-Aldrich) and wait for 10 min.
5. Pipette 5-10 μ l of sample from the bottom of the vial, and sandwich between two cover slips. This sample, containing a large number of temporarily immobilized worms (e.g. 50-100 worms), can be placed on the detector to start data acquisition.

3. Data Acquisition

Here, we summarize the image acquisition steps for a typical LOT experiment, which was automated by using a custom developed LabView interface.

1. Adjust the initial angle of the rotation stage to -50° , where 0° corresponds to the vertical position of the light source.
2. Adjust the initial position of the X-Y stage to (0,0), which is the HOME position.
3. Adjust the exposure time of the detector to best utilize its dynamic range such that the image is as bright as possible without any saturated pixels.
4. Without changing the angle of the rotation stage, capture 9 images. For each image, move the X-Y stage to a new position in a 3x3 square grid such that each image shifts by approximately one quarter of a pixel compared to the previous one. Acquiring more images at each angle, e.g. in a 6 μ 6 grid, might improve resolution depending on the type of the object and signal-to-noise ratio (SNR).¹⁰
5. Adjust the initial position of the X-Y stage to (0,0), which is the HOME position.
6. Increase the angle of the rotation stage by increments of 2° , until reaching $+50^\circ$. After each increment, i.e. at each new angle, repeat steps 3-5. The angular increments can be finer or coarser depending on the optimization of acquisition time vs. imaging resolution.
7. (Optional step if a dual-axis tomography scheme is to be utilized) Rotate the horizontal stage on which the detector is mounted by 90° . Then, repeat steps 1-6.

4. Data Analysis

Following the steps 1-6 in Section 3, a set of 459 images is acquired, which contains 9 sub-pixel shifted images for each of the 51 different angles of illumination. First, each set of 9 images is digitally processed, using pixel super-resolution algorithms¹⁰, to obtain one high-resolution (HR) projection hologram per angle. It should be noted that pixel super-resolution refers to overcoming the limitation of the pixel size, rather than the diffraction limit, on the spatial resolution of lensfree images. Pixel super-resolved holograms are then digitally reconstructed⁷⁻¹⁰ to obtain 51 projection images. This set of 51 projection images is then back-projected using TomoJ, a plug-in for ImageJ (an open source image analysis software).¹¹ This back-projection operation outputs a three-dimensional image (tomograms) of the sample. Although not implemented here, a dual-axis tomography scheme could also be utilized as described in Ref. 7. In this scheme, a second set of tomograms is obtained by rotating the light source along an orthogonal axis with respect to the first rotation axis, which provides more spatial information regarding the sample, and improves axial resolution.

5. Representative Results

The large field-of-view (FOV) of lensfree optical tomography is demonstrated in **Figure 1**. As the sample is placed directly on the top of the detector-array, holographic images of the objects can be recorded over a FOV of 24 mm², which can be further increased using emerging detector arrays with larger active areas.

Although pixel size of the detector-array limits the resolution of the recorded holographic images, pixel super-resolution techniques mitigate this problem. **Figure 2** shows pixel super-resolved holograms along with the reconstructed images (i.e. projection images) that offer sub-micrometer spatial resolution, for three different angles of illumination.

The projection images can be combined using tomographic image reconstruction techniques (e.g. filtered back-projection) to compute tomograms (i.e. three dimensional images) of the specimen. **Figure 3** shows three slice images in the x-y plane through the anterior of the worm, where the pharyngeal tube is visible only in the slice through $z=8 \mu\text{m}$, as expected from this roughly cylindrical structure with $\sim 5 \mu\text{m}$ outer diameter. Moreover, the cross-sectional image in the x-z plane (inset in **Figure 3** top panel) clearly shows the boundaries of the worm and the pharyngeal tube inside (pointed by the arrows), demonstrating successful 3D imaging of the pharynx.

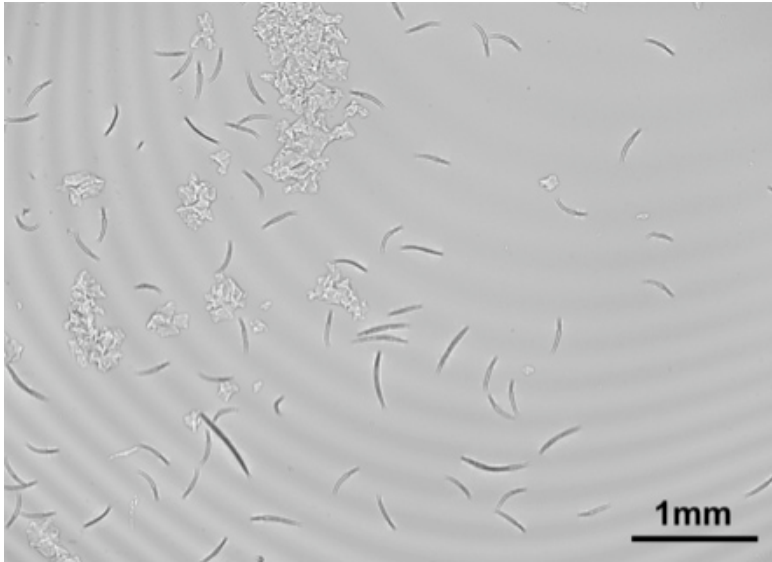


Figure 1 shows a full field-of-view (24 mm^2) holographic image recorded using the lensfree optical tomography (LOT) setup for vertical illumination. Owing to the large imaging area of LOT, many worms can be simultaneously imaged with a single data acquisition step.

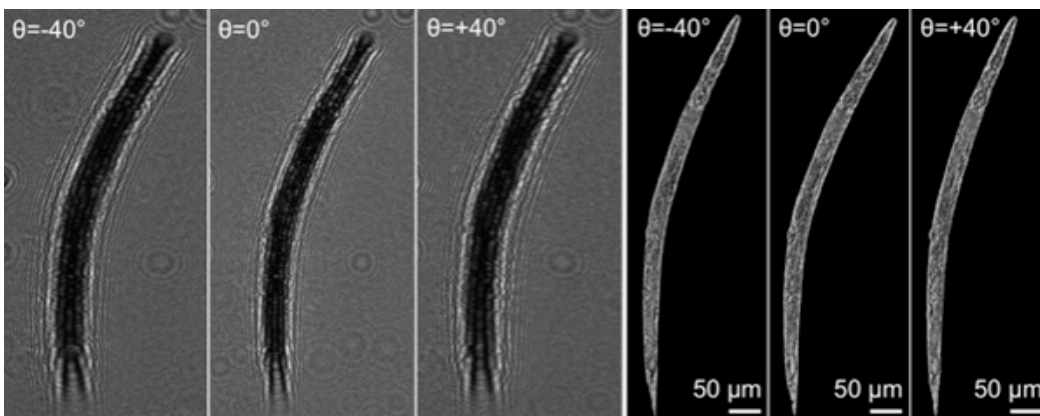


Figure 2 shows the pixel super-resolved holograms (left panel) and the digitally reconstructed projection images (right panel) for a *C. elegans* worm (cropped from a large field-of-view) at three different illumination angles. Each projection image contains information regarding a different viewing angle, which enables computation of the 3D structure through a filtered back-projection operation.

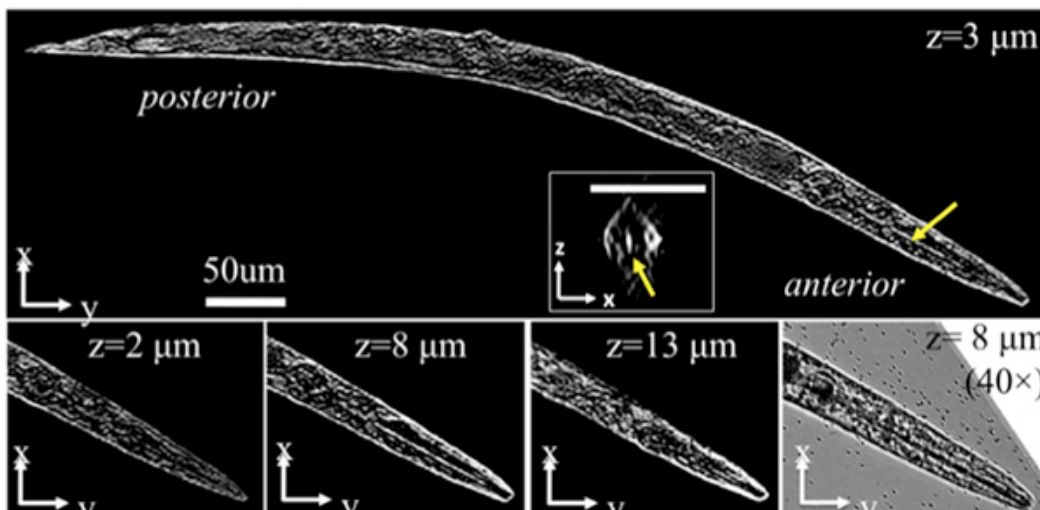


Figure 3 shows computed tomograms for the *C. elegans* worm of **Figure 2**. (Top row) shows a slice image of the entire worm at $z=3\ \mu\text{m}$. The inset shows a cross-sectional image from the anterior of the worm. Scale bar of the inset is $50\ \mu\text{m}$. (Bottom row) Shows three slice images through the anterior of the worm, demonstrating the optical sectioning ability of lensfree optical tomography. Arrows throughout the figure indicate the same point on the pharyngeal tube of the worm. A microscope image ($\times 40$, 0.65-NA) is also provided for visual comparison.

Discussion

It is important to emphasize that the unique geometry of lensfree on-chip holographic microscopy is the critical enabler to achieve pixel super-resolution and tomographic imaging. Since the recorded images are not assumed to be projection images as in incoherent contact imaging approaches¹², but *projection holograms*, the diffraction of the transmitted light until it impinges on the detector can be digitally corrected by holographic reconstruction. Therefore, variations in the sample-to-sensor distance can be accounted. Moreover, since the sample-to-sensor distance is typically $\sim 0.5\text{-}5\ \text{mm}$, while the light source is placed at $\sim 4\text{-}10\ \text{cm}$ distance from the sample, achieving sub-pixel shifts does not require large source shifts. As a result, moving the light source only by $50\text{-}100\ \mu\text{m}$ is sufficient to achieve sub-pixel shifts at the detector plane, preventing undesired variations in *i)* illumination direction/perspective, and *ii)* effective sample-to-sensor distance at each source position. If not prevented, these variations could cause significant aberrations in the pixel super-resolved images. Therefore, the holograms recorded at each source position, at a given angle, can actually be considered to be sub-pixel shifted versions of the same holographic image. Moreover, the almost alignment-free design of lensfree optical tomography makes it rather straightforward to record projection holograms at different angles, simply by rotating a light source^{7,9}, or using multiple light sources (such as LEDs) at different angles⁸.

LOT is an emerging technique that offers a large space-bandwidth product for on-chip imaging of samples. Importantly, it is a scalable technology that will greatly benefit from the next generation detector arrays. That is, as faster CMOS and CCD detector arrays with denser pixels become available, LOT will continuously improve both in terms of resolution, field-of-view and speed. This is an important advantage of lensfree on-chip microscopy over conventional light microscopy, where imaging performance is determined by multiple sub-systems, impeding the direct scaling of image quality with the advances in digital technologies.

In summary, enabling high-throughput 3D microscopy of specimens over a large imaging volume, in a compact architecture, lensfree optical tomography can be a useful toolset for lab-on-a-chip systems.

Disclosures

No conflicts of interest declared.

References

1. Schmitt, J.M. Optical coherence tomography (OCT): a review, *J. Sel. Top. In: Quant. Elect.*, **Vol. 5**, 1205-1215, (1999).
2. Keller, P.J., A.D. Schmidt, J., & Wittbrodt, E.H.K. Stelzer, Reconstruction of zebrafish early embryonic development by scanned light sheet microscopy. *Science*. **322**, 1065-1069 (2008).
3. Sharpe, J., Ahlgren, U., Perry, P., Hill, B., Ross, A., Hecksher-Sørensen, J., Baldock, R., & Davidson, D. Optical Projection Tomography as a Tool for 3D Microscopy and Gene Expression Studies. *Science*. **296**, 541-545 (2002).
4. Sung, Y., Choi, W., Fang-Yen, C., Badizadegan, K., Dasari, R.R., & Feld, M.S. Optical diffraction tomography for high resolution live cell imaging. *Opt. Exp.* **17**, 266-277 (2009).
5. Debailleul, M., Simon, B., Georges, V., Haeberle, O., & Lauer, V. Holographic microscopy and diffractive microtomography of transparent samples. *Meas. Sci. Technol.* **19**, 074009 (2008).
6. Charrière, F., Pavillon, N., Colomb, T., Depeursinge, C., Heger, T.J., Mitchell, E.A.D., Marquet, P., & Rappaz, B. Living specimen tomography by digital holographic microscopy: Morphometry of testate amoeba. *Opt. Exp.* **14**, 7005-7013 (2006).
7. Isikman, S.O., Bishara, W., Mavandadi, S., Yu, S.W., Feng, S., Lau, R., & Ozcan, A. Lens-free optical tomographic microscope with a large imaging volume on a chip. *Proc. Nat. Acad. Sci.* **108**, 7296-7301 (2011).
8. Isikman, S.O., Bishara, W., Sikora, U., Yaglidere, O., Yeah, J., & Ozcan, A. Field-portable Lensfree Tomographic Microscope. *Lab Chip*. **11**, 2222-2230 (2011).
9. Isikman, S.O., Bishara, W., Zhu, H., & Ozcan, A. Optofluidic tomography on a chip. *App. Phys. Lett.* **98**, 161109 (2011).
10. Bishara, W., Su, T.W., Coskun, A., & Ozcan, A. Lensfree on-chip microscopy over a wide field-of-view using pixel super-resolution. *Opt. Exp.* **18**, 11181-11191 (2010).
11. Messaoudi, C., Boudier, T., Sorzano, C.O.S., & Marco, S. TomoJ: tomography software for three-dimensional reconstruction in transmission electron microscopy. *BMC Bioinformatics*. **8**, 288 (2007).
12. Heng, X., Erickson, D., Baugh, L. R., Yaqoob, Z., Sternberg, P.W., Psaltis, D., & Yang, C. Optofluidic Microscopy: A Method for Implementing High Resolution Optical Microscope On A Chip. *Lab on a Chip*. **6**, 1274-1276 (2006).